J. Fluid Mech. (1995), *vol.* 292, *pp.* 359–376

Pressure-driven flow of a thin viscous sheet

By B. W. VAN DE FLIERT, P. D. HOWELL AND J. R. OCKENDEN

Mathematical Institute, 24–29 St Giles', Oxford, UK

(Received 8 August 1994 and in revised form 12 January 1995)

Systematic asymptotic expansions are used to find the leading-order equations for the pressure-driven flow of a thin sheet of viscous fluid. Assuming the fluid geometry to be slender with non-negligible curvatures, the Navier–Stokes equations with appropriate free-surface conditions are simplified to give a 'shell-theory' model. The fluid geometry is not known in advance and a time-dependent coordinate frame has to be employed. The effects of surface tension, gravity and inertia can also be incorporated in the model.

1. Introduction

This paper is motivated by the continuing need for systematic reductions of the Navier–Stokes equations for the flow of viscous fluids with free boundaries in high-aspect-ratio configurations. While there is a burgeoning literature concerning the modelling of nearly one-dimensional fibres in many different configurations (Matovich & Pearson 1969; Pearson & Matovich 1969; Shah & Pearson 1972; Geyling 1976; Geyling & Homsy 1980; Schultz & Davis 1982; Dewynne, Ockendon & Wilmott 1989, 1992; Dewynne, Howell & Wilmott 1994), the theory of fluid sheets is much less well-developed mathematically (Pearson & Petrie 1970*a*,*b*; Yeow 1976; Buckmaster, Nachman & Ting 1975; Buckmaster & Nachman 1978; Wilmott 1989; Yarin, Gospodinov & Roussinov 1994; much background literature can be found in the book of Pearson 1985). Many of these authors were studying the process of film-blowing and in particular the phenomenon of draw-resonance and hence there has been an emphasis on steady axisymmetric flow and its linear stability. The basic model for isoviscous Newtonian flow introduced by Pearson & Petrie (1970*a*) works with intrinsic coordinates tailored to the unknown steady film surface; later generalizations cover non-Newtonian and viscoelastic films (Gupta, Metzner & Wissbrun 1982; Cao & Campbell 1990) and a nonlinear evolution model has been considered briefly by Yarin *et al.* (1994). In this paper we have been motivated by flows occurring in glass bottle manufacture to try to write down a self-consistent derivation of some models for general unsteady pressure-driven flows in arbitrarily curved sheets, with the hope that the predictions of these models can be compared to the CFD codes that are currently used in the glass industry (Saxelby & Aitchison 1986; Burley & Graham 1991; Graham *et al.* 1992). Thus our model stands in the same relation to that of Pearson & Petrie (1970*a*) as do the evolution models for fibre-drawing (such as Dewynne *et al.* 1989) to the steady draw-down theory of Matovich & Pearson (1969) and Shah & Pearson (1972).

The idea of using simplified 'thin geometry' models has been exploited extensively in solid mechanics and we may expect the models we derive to be closely

related, modulo a time derivative, to those for plates and shells (see for instance Love 1927; Landau & Lifschitz 1959; Timoshenko & Woinowsky-Krieger 1959). For steady flows this point has already been made in Pearson & Petrie (1970*a*), but there is one important modelling difference between the fluid and solid mechanics situations: viscous liquid sheets can readily undergo deformations, in particular extensions, that for solids would be large enough to demand mechanical nonlinearity and/or plastic flow in addition to geometric nonlinearity.

The relative ease with which fluid sheets can be modelled in certain symmetric configurations will enable us to make some general statements about the response of a sheet to normal forces in terms of finite-time blow-up, history-dependence and analogies between one- and two-dimensional flow.

The plan of the paper is to derive the basic sheet model in § 2, using tailored curvilinear coordinates and assuming a balance between the external forces and viscous stresses in the fluid. With the problem of bottle-blowing in mind, we include the effect of an imposed pressure drop across the sheet. This model is then analysed in § 3 for certain symmetric geometries. In particular we demonstrate blow-up behaviour and give some numerical solutions in certain parameter regimes of relevance in bottle manufacture. In the Appendix we extend the theory to include the effects of surface tension, gravity and inertia, still excluding other practically important mechanisms such as heat transfer and contact between the sheet and a containing boundary.

1.1. *Parameter regimes*

Glass compositions vary quite substantially, depending on the purpose of the glass product. Typically for bottles the glass is made from approximately 75% silica, 15% soda and 10% lime. The different parameters in the model depend largely on the composition and the circumstances, in particular the temperatures in the process, which may vary from 600°C to 1100°C. For the production of glass containers or bottles the parameters are of the order (see Graham 1987 and references therein):

surface tension:	$\gamma \sim 0.3\ \mathrm{N\,m^{-1}}$,	density :	$\rho \sim 2500\ \mathrm{kg\,m^3}$,
pressure drop :	$\Delta P \sim 7000\ \mathrm{Pa}$,	viscosity :	$\mu \sim 10^2 - 10^8\ \mathrm{N\,s\,m^{-2}}$,
radius :	$L \sim 0.02 - 0.1\ \mathrm{m}$,	thickness :	$h \sim 0.003 - 0.015\ \mathrm{m}$.

With a length scale $L = 6$ cm and thickness $h = 0.5$ cm, a typical aspect ratio is given by $\varepsilon = h/L = 0.1$. Of course the aspect ratio changes considerably during the blowing process and the variation in μ can result in large deviations in the Reynolds number. With a typical velocity given by $U = L\Delta P/\varepsilon\mu$, the dimensionless parameters are

$$Re = \frac{\rho L^2 \Delta P}{\varepsilon \mu^2} \sim 10^{-10} - 10^2, \quad \gamma^* = \frac{\gamma}{L\Delta P} \sim 10^{-4}, \quad St = \frac{\rho g L \varepsilon}{\Delta P} \sim 10^{-2}.$$

The order of the parameters motivates us to consider the Stokes equations for slow viscous flow, neglecting inertia, surface tension and gravity for most of this paper. These other effects will be considered briefly in the Appendix.

2. The dynamics of curved viscous sheets

We consider the dynamics of a general slender sheet of viscous fluid where the curvature of the sheet is not small. We follow Yeow (1976) and Pearson (1985, §8.2), for example, and choose a coordinate system fixed in the fluid sheet, supposing the centre-surface of the sheet to be given by

$$\boldsymbol{r} = \boldsymbol{r}_c(x_1, x_2, t),$$

where x_1 and x_2 are spatial parameters and t is time. The unit normal to this surface is given by

$$\boldsymbol{n} = \left|\frac{\partial \boldsymbol{r}_c}{\partial x_1} \wedge \frac{\partial \boldsymbol{r}_c}{\partial x_2}\right|^{-1} \left(\frac{\partial \boldsymbol{r}_c}{\partial x_1} \wedge \frac{\partial \boldsymbol{r}_c}{\partial x_2}\right). \tag{2.1}$$

As noted in Pearson (1985, §8.2), this coordinate system is time-dependent and, at present, largely arbitrary. However our analysis is based upon the simplifications which are obtained when we choose to parametrize the sheet in such a way that lines of constant x_1 and x_2 are lines of principal curvature† of the centre-surface $\boldsymbol{r} = \boldsymbol{r}_c$, so that with respect to these parameters the first and second fundamental forms of the surface are orthogonal (see e.g. Kreyszig 1959). Hence we may define an orthonormal basis $\{\boldsymbol{e}_1, \boldsymbol{e}_2, \boldsymbol{n}\}$, where

$$\boldsymbol{e}_1 = \frac{1}{a_1}\frac{\partial \boldsymbol{r}_c}{\partial x_1}, \quad \boldsymbol{e}_2 = \frac{1}{a_2}\frac{\partial \boldsymbol{r}_c}{\partial x_2}, \quad \text{with } a_1 = \left|\frac{\partial \boldsymbol{r}_c}{\partial x_1}\right|, \quad a_2 = \left|\frac{\partial \boldsymbol{r}_c}{\partial x_2}\right|, \tag{2.2}$$

and the derivatives of $\boldsymbol{n}$ are given by

$$\frac{\partial \boldsymbol{n}}{\partial x_1} = -\kappa_1 a_1 \boldsymbol{e}_1 \quad \text{and} \quad \frac{\partial \boldsymbol{n}}{\partial x_2} = -\kappa_2 a_2 \boldsymbol{e}_2, \tag{2.3}$$

where κ_i are the principal curvatures. We shall be using the coordinates (x_1, x_2, n) to describe a general point of the fluid sheet whose position is given by

$$\boldsymbol{r} = \boldsymbol{r}_c + n\boldsymbol{n}. \tag{2.4}$$

Using (2.3) we see that this coordinate system is orthogonal, with metric $l_1^2 dx_1^2 + l_2^2 dx_2^2 + l_3^2 dx_3^2$, where

$$l_1 = a_1(1 - \kappa_1 n), \quad l_2 = a_2(1 - \kappa_2 n), \quad l_3 = 1. \tag{2.5}$$

The velocity of the centre-surface $\boldsymbol{r} = \boldsymbol{r}_c$ is

$$\frac{\partial \boldsymbol{r}_c}{\partial t} = v_1 \boldsymbol{e}_1 + v_2 \boldsymbol{e}_2 + v_3 \boldsymbol{n}. \tag{2.6}$$

Finally, by differentiating (2.2) and (2.3) with respect to x_1 and x_2, we have the usual differential geometry relations between a_i and κ_i:

$$a_1 \frac{\partial \kappa_1}{\partial x_2} = (\kappa_2 - \kappa_1)\frac{\partial a_1}{\partial x_2}, \quad a_2 \frac{\partial \kappa_2}{\partial x_1} = (\kappa_1 - \kappa_2)\frac{\partial a_2}{\partial x_1}, \tag{2.7}$$

$$\frac{\partial}{\partial x_1}\left(\frac{1}{a_1}\frac{\partial a_2}{\partial x_1}\right) + \frac{\partial}{\partial x_2}\left(\frac{1}{a_2}\frac{\partial a_1}{\partial x_2}\right) + a_1 a_2 \kappa_1 \kappa_2 = 0, \tag{2.8}$$

((2.8) is the so-called Gauss characteristic equation), while differentiation of (2.6) gives three relations for the velocity components of the centre-surface:

$$a_2 \frac{\partial a_1}{\partial t} = a_2 \frac{\partial v_1}{\partial x_1} + v_2 \frac{\partial a_1}{\partial x_2} - a_1 a_2 \kappa_1 v_3, \tag{2.9}$$

$$a_1 \frac{\partial a_2}{\partial t} = a_1 \frac{\partial v_2}{\partial x_2} + v_1 \frac{\partial a_2}{\partial x_1} - a_1 a_2 \kappa_2 v_3, \tag{2.10}$$

† At an umbilic point of the surface, where the principal curvatures are equal, these lines are not uniquely defined and at an isolated umbilic our model will possess spurious singular solutions.

and

$$v_1\frac{\partial a_1}{\partial x_2}+v_2\frac{\partial a_2}{\partial x_1}=a_1\frac{\partial v_1}{\partial x_2}+a_2\frac{\partial v_2}{\partial x_1}. \tag{2.11}$$

2.1. *Non-dimensionalization and scaling*

We non-dimensionalize the equations so as to exploit the slenderness of the sheet. We suppose L is a typical length scale for the sheet, say a typical radius of curvature, while εL is a (much smaller) typical thickness. We allow for varying viscosity, but suppose that it is typically of order M. We denote by (u_1, u_2, u_3) the fluid velocities in the $\boldsymbol{e}_1$-, $\boldsymbol{e}_2$- and $\boldsymbol{n}$-directions. The scalings we employ are

$$\left.\begin{array}{lllll} x_1 = Lx_1', & t = \Delta P^{-1}\varepsilon M t', & u_1 = L\Delta P\varepsilon^{-1}M^{-1}u_1', & a_1 = a_1', & \kappa_1 = L^{-1}\kappa_1', \\ x_2 = Lx_2', & \boldsymbol{r}_c = L\boldsymbol{r}_c', & u_2 = L\Delta P\varepsilon^{-1}M^{-1}u_2', & a_2 = a_2', & \kappa_2 = L^{-1}\kappa_2', \\ n = \varepsilon L n', & h = \varepsilon L h', & u_3 = L\Delta P\varepsilon^{-1}M^{-1}u_3', & \mu = M\mu', & p = \Delta P\varepsilon^{-1}p'. \end{array}\right\} \tag{2.12}$$

Without loss of generality we have supposed x_1 and x_2 to have dimensions of length and the time scale has been chosen to be $LU^{-1} = \Delta P^{-1}\varepsilon M$. Other consistent scalings are also possible, in particular on shorter timescales, and we will return to this point in the conclusion.

These scalings are used to non-dimensionalize the Stokes equations and boundary conditions. Solutions are sought in the form of asymptotic expansions in powers of the slenderness parameter ε, typically (dropping primes)

$$u_1 \sim u_1^{(0)} + \varepsilon u_1^{(1)} + \varepsilon^2 u_1^{(2)} + \cdots.$$

2.2. *The Stokes equations and boundary conditions*

Employing (2.12), the metric (2.5) is rescaled to

$$l_1 = a_1(1-\varepsilon\kappa_1 n), \quad l_2 = a_2(1-\varepsilon\kappa_2 n), \quad l_3 = 1.$$

The incompressibility condition may be written

$$\frac{\partial}{\partial x_1}(l_2u_1)+\frac{\partial}{\partial x_2}(l_1u_2)+\frac{1}{\varepsilon}\frac{\partial}{\partial n}(l_1l_2u_3)=0, \tag{2.13}$$

and force balances in the $\boldsymbol{e}_1$-, $\boldsymbol{e}_2$- and $\boldsymbol{n}$-directions are (see e.g. Aris 1962; Rosenhead 1963)

$$\frac{\partial}{\partial x_1}(l_2\sigma_{11})+\frac{\partial}{\partial x_2}(l_1\sigma_{12})+\frac{\partial l_1}{\partial x_2}\sigma_{12}+\frac{1}{\varepsilon}\frac{\partial}{\partial n}(l_1l_2\sigma_{13})+\frac{l_2}{\varepsilon}\frac{\partial l_1}{\partial n}\sigma_{13}-\frac{\partial l_2}{\partial x_1}\sigma_{22}=0, \tag{2.14}$$

$$\frac{\partial}{\partial x_1}(l_2\sigma_{12})+\frac{\partial}{\partial x_2}(l_1\sigma_{22})+\frac{\partial l_2}{\partial x_1}\sigma_{12}+\frac{1}{\varepsilon}\frac{\partial}{\partial n}(l_1l_2\sigma_{23})+\frac{l_1}{\varepsilon}\frac{\partial l_2}{\partial n}\sigma_{23}-\frac{\partial l_1}{\partial x_2}\sigma_{11}=0, \tag{2.15}$$

$$\frac{\partial}{\partial x_1}(l_2\sigma_{13})+\frac{\partial}{\partial x_2}(l_1\sigma_{23})+\frac{1}{\varepsilon}\frac{\partial}{\partial n}(l_1l_2\sigma_{33})-\frac{l_2}{\varepsilon}\frac{\partial l_1}{\partial n}\sigma_{11}-\frac{l_1}{\varepsilon}\frac{\partial l_2}{\partial n}\sigma_{22}=0. \tag{2.16}$$

The stress is given by

$$\sigma_{11} = -p+\frac{2\mu}{l_1}\left(\frac{\partial u_1}{\partial x_1}+\frac{u_2}{l_2}\frac{\partial l_1}{\partial x_2}+\frac{u_3}{\varepsilon}\frac{\partial l_1}{\partial n}\right), \tag{2.17}$$

$$\sigma_{22} = -p + \frac{2\mu}{l_2}\left(\frac{\partial u_2}{\partial x_2} + \frac{u_1}{l_1}\frac{\partial l_2}{\partial x_1} + \frac{u_3}{\varepsilon}\frac{\partial l_2}{\partial n}\right), \tag{2.18}$$

$$\sigma_{33} = -p + \frac{2\mu}{\varepsilon}\frac{\partial u_3}{\partial n}, \tag{2.19}$$

$$\sigma_{12} = \frac{\mu}{l_1 l_2}\left(l_1\frac{\partial u_1}{\partial x_2} - \frac{\partial l_1}{\partial x_2}u_1 + l_2\frac{\partial u_2}{\partial x_1} - \frac{\partial l_2}{\partial x_1}u_2\right), \tag{2.20}$$

$$\sigma_{13} = \frac{\mu}{l_1}\left(\frac{l_1}{\varepsilon}\frac{\partial u_1}{\partial n} - \frac{u_1}{\varepsilon}\frac{\partial l_1}{\partial n} + \frac{\partial u_3}{\partial x_1}\right), \tag{2.21}$$

$$\sigma_{23} = \frac{\mu}{l_2}\left(\frac{l_2}{\varepsilon}\frac{\partial u_2}{\partial n} - \frac{u_2}{\varepsilon}\frac{\partial l_2}{\partial n} + \frac{\partial u_3}{\partial x_2}\right). \tag{2.22}$$

On the free boundaries, given by $n = \pm\frac{1}{2}h$, we impose stress conditions, incorporating the effect of a pressure drop across the sheet, with $P_\pm$ the pressures applied to the surfaces:

$$\sigma_{13} = \pm\frac{\varepsilon}{2l_1}\frac{\partial h}{\partial x_1}\sigma_{11} \pm \frac{\varepsilon}{2l_2}\frac{\partial h}{\partial x_2}\sigma_{12}, \tag{2.23}$$

$$\sigma_{23} = \pm\frac{\varepsilon}{2l_1}\frac{\partial h}{\partial x_1}\sigma_{12} \pm \frac{\varepsilon}{2l_2}\frac{\partial h}{\partial x_2}\sigma_{22}, \tag{2.24}$$

$$\sigma_{33} = \pm\frac{\varepsilon}{2l_1}\frac{\partial h}{\partial x_1}\sigma_{13} \pm \frac{\varepsilon}{2l_2}\frac{\partial h}{\partial x_2}\sigma_{23} - \varepsilon P_\pm. \tag{2.25}$$

Using the expression for the convective derivative

$$\frac{\mathrm{D}\phi}{\mathrm{D}t} = \frac{\partial\phi}{\partial t} + \left(\boldsymbol{u} - \frac{\partial \boldsymbol{r}_c}{\partial t} - n\frac{\partial \boldsymbol{n}}{\partial t}\right)\cdot\nabla\phi, \tag{2.26}$$

the kinematic condition may be written in the form

$$\begin{aligned} u_3 - v_3 = \pm\frac{\varepsilon}{2}\frac{\partial h}{\partial t} &\pm \frac{\varepsilon}{2l_1}\frac{\partial h}{\partial x_1}\left[u_1 - v_1 \pm \frac{\varepsilon h}{2}\left(\kappa_1 v_1 + \frac{1}{a_1}\frac{\partial v_3}{\partial x_1}\right)\right] \\ &\pm \frac{\varepsilon}{2l_2}\frac{\partial h}{\partial x_2}\left[u_2 - v_2 \pm \frac{\varepsilon h}{2}\left(\kappa_2 v_2 + \frac{1}{a_2}\frac{\partial v_3}{\partial x_2}\right)\right]. \end{aligned} \tag{2.27}$$

2.3. *Leading-order equations*

When we formally set $\varepsilon = 0$ in (2.13)–(2.27) we see that the resulting homogeneous equations and boundary conditions admit eigensolutions in which $\boldsymbol{u}^{(0)}$ is independent of n and $u_3^{(0)} = v_3^{(0)}$. The apparent indeterminacy in the leading-order unknowns is resolved by proceeding to higher order in the asymptotic expansion. This results in inhomogeneous versions of the leading-order problems. By the Fredholm alternative, these inhomogeneous problems have no solutions unless certain orthogonality conditions are met and it is these solvability conditions that provide us with a closed system of equations for the leading-order unknowns.

Indeed, from (2.25) we expect to have to proceed to terms of $O(\varepsilon^2)$ if we are to discern the effect of the driving pressure. The terms of $O(\varepsilon)$ in the continuity equation and kinematic condition give

$$u_3^{(1)} - v_3^{(1)} = \frac{n}{a_1^{(0)}a_2^{(0)}}\left(a_1^{(0)}a_2^{(0)}(\kappa_1^{(0)} + \kappa_2^{(0)})u_3^{(0)} - \frac{\partial}{\partial x_1}(a_2^{(0)}u_1^{(0)}) - \frac{\partial}{\partial x_2}(a_1^{(0)}u_2^{(0)})\right), \tag{2.28}$$

and, after rearrangement, the averaged conservation of mass equation:

$$\frac{\partial}{\partial t}(a_1^{(0)}a_2^{(0)}h^{(0)}) + \frac{\partial}{\partial x_1}[a_2^{(0)}h^{(0)}(u_1^{(0)} - v_1^{(0)})] + \frac{\partial}{\partial x_2}[a_1^{(0)}h^{(0)}(u_2^{(0)} - v_2^{(0)})] = 0. \tag{2.29}$$

Then (2.16) with (2.25) can be solved for $p^{(0)}$:

$$p^{(0)} = \frac{2\mu^{(0)}}{a_1^{(0)}a_2^{(0)}}\left(a_1^{(0)}a_2^{(0)}(\kappa_1^{(0)} + \kappa_2^{(0)})v_3^{(0)} - \frac{\partial}{\partial x_1}(a_2^{(0)}u_1^{(0)}) - \frac{\partial}{\partial x_2}(a_1^{(0)}u_2^{(0)})\right), \tag{2.30}$$

and (2.14), (2.15) with (2.23), (2.24) give

$$u_1^{(1)} = F_1(x_1, x_2, t) - n\left(\kappa_1^{(0)}u_1^{(0)} + \frac{1}{a_1^{(0)}}\frac{\partial v_3^{(0)}}{\partial x_1}\right), \tag{2.31}$$

$$u_2^{(1)} = F_2(x_1, x_2, t) - n\left(\kappa_2^{(0)}u_2^{(0)} + \frac{1}{a_2^{(0)}}\frac{\partial v_3^{(0)}}{\partial x_2}\right), \tag{2.32}$$

for some arbitrary functions F_1 and F_2. Thus the Fredholm alternative does not close the model even at this order of approximation and we must proceed to terms of $O(\varepsilon^2)$. Following the above procedure, (2.16) and (2.25) yield

$$\frac{\partial \sigma_{33}^{(1)}}{\partial n} + \kappa_1^{(0)}\sigma_{11}^{(0)} + \kappa_2^{(0)}\sigma_{22}^{(0)} = 0, \tag{2.33}$$

with

$$\sigma_{33}^{(1)} = -P_{\pm} \text{ on } n = \pm\tfrac{1}{2}h^{(0)}, \tag{2.34}$$

and hence the transverse stress balance is

$$\kappa_1^{(0)}\bar{\sigma}_{11}^{(0)} + \kappa_2^{(0)}\bar{\sigma}_{22}^{(0)} + P_- - P_+ = 0, \tag{2.35}$$

where the bar denotes averaging from $n = -\frac{1}{2}h$ to $n = +\frac{1}{2}h$; this stress balance is just the first of the aforementioned solvability conditions demanded by the Fredholm alternative. The equations (2.33) and (2.34) can now be solved for $p^{(1)}$. Similarly (2.14) and (2.15) prescribe the n-derivatives of $\sigma_{13}^{(1)}$ and $\sigma_{23}^{(1)}$ and these may be integrated using the terms of $O(\varepsilon^2)$ in (2.23) and (2.24). The details of this straightforward but lengthy calculation can be found in Howell (1994) and here we simply record the other solvability conditions in (2.40) and (2.41), given in a form which emphasizes the analogy with the shell equations of linear elasticity. Defining the relative velocities

$$\tilde{u}_1 = u_1 - v_1 \quad \text{and} \quad \tilde{u}_2 = u_2 - v_2,$$

and using the relations (2.7)–(2.11), the leading-order forms of (2.17), (2.18) and (2.20) are (dropping superscripts $^{(0)}$)

$$\bar{\sigma}_{11} = \frac{2\mu h}{a_1 a_2}\left[2\left(a_2\frac{\partial a_1}{\partial t} + \tilde{u}_2\frac{\partial a_1}{\partial x_2} + a_2\frac{\partial \tilde{u}_1}{\partial x_1}\right) + \left(a_1\frac{\partial a_2}{\partial t} + \tilde{u}_1\frac{\partial a_2}{\partial x_1} + a_1\frac{\partial \tilde{u}_2}{\partial x_2}\right)\right], \tag{2.36}$$

$$\bar{\sigma}_{22} = \frac{2\mu h}{a_1 a_2}\left[\left(a_2\frac{\partial a_1}{\partial t} + \tilde{u}_2\frac{\partial a_1}{\partial x_2} + a_2\frac{\partial \tilde{u}_1}{\partial x_1}\right) + 2\left(a_1\frac{\partial a_2}{\partial t} + \tilde{u}_1\frac{\partial a_2}{\partial x_1} + a_1\frac{\partial \tilde{u}_2}{\partial x_2}\right)\right], \tag{2.37}$$

$$\bar{\sigma}_{12} = \frac{\mu h}{a_1 a_2}\left[a_1\frac{\partial \tilde{u}_1}{\partial x_2} + a_2\frac{\partial \tilde{u}_2}{\partial x_1}\right], \tag{2.38}$$

and (2.29) becomes

$$\frac{\partial}{\partial t}(a_1 a_2 h) + \frac{\partial}{\partial x_1}(\tilde{u}_1 a_2 h) + \frac{\partial}{\partial x_2}(\tilde{u}_2 a_1 h) = 0; \tag{2.39}$$

the consequence of the derivation mentioned above is the tangential force balance

$$\frac{\partial}{\partial x_1}(a_2 \bar{\sigma}_{11}) + \frac{\partial}{\partial x_2}(a_1 \bar{\sigma}_{12}) + \frac{\partial a_1}{\partial x_2}\bar{\sigma}_{12} - \frac{\partial a_2}{\partial x_1}\bar{\sigma}_{22} = 0, \tag{2.40}$$

and

$$\frac{\partial}{\partial x_1}(a_2 \bar{\sigma}_{12}) + \frac{\partial}{\partial x_2}(a_1 \bar{\sigma}_{22}) + \frac{\partial a_2}{\partial x_1}\bar{\sigma}_{12} - \frac{\partial a_1}{\partial x_2}\bar{\sigma}_{11} = 0. \tag{2.41}$$

The equations (2.35), (2.39)–(2.41), (2.7) and (2.8) form a closed system of seven equations for the unknowns $h, \kappa_1, \kappa_2, a_1, a_2, \tilde{u}_1, \tilde{u}_2$. We note that (2.35), (2.40) and (2.41) are identical to the equilibrium equations of classical shell theory (see Love 1927, art. 331). However, in our formulation neither the thickness nor the geometry of the sheet is prescribed in advance. One possible procedure for determining the evolution of this geometry is to (i) assume we know the variables $h, \kappa_1, \kappa_2, a_1, a_2$ at an instant of time, (ii) compute the stresses with a 'shell theory' calculation from (2.35), (2.40) and (2.41) and (iii) update the geometry via the evolution equations (2.36), (2.37) and (2.39).

3. Symmetric geometries

The difficulties associated with the evolution of the geometrical variables can be minimised if symmetries can be exploited and we shall demonstrate this for planar, axisymmetric and for purely two-dimensional sheets.

3.1. *Planar and nearly planar sheets*

It is tempting to consider the case of a flat centre-surface so that for all time,

$$a_1 = a_2 = 1, \quad \kappa_2 = \kappa_2 = 0.$$

In this case we could, from (2.39)–(2.41), retrieve a closed system comprising an evolution equation for h coupled to a second-order elliptic system for $\tilde{u}_1, \tilde{u}_2$:

$$\frac{\partial h}{\partial t} + \frac{\partial}{\partial x_1}(\tilde{u}_1 h) + \frac{\partial}{\partial x_2}(\tilde{u}_2 h) = 0, \tag{3.1}$$

$$\frac{\partial}{\partial x_1}\left(2\mu h(2\frac{\partial \tilde{u}_1}{\partial x_1} + \frac{\partial \tilde{u}_2}{\partial x_2})\right) + \frac{\partial}{\partial x_2}\left(\mu h(\frac{\partial \tilde{u}_1}{\partial x_2} + \frac{\partial \tilde{u}_2}{\partial x_1})\right) = 0, \tag{3.2}$$

$$\frac{\partial}{\partial x_1}\left(\mu h(\frac{\partial \tilde{u}_1}{\partial x_2} + \frac{\partial \tilde{u}_2}{\partial x_1})\right) + \frac{\partial}{\partial x_2}\left(2\mu h(\frac{\partial \tilde{u}_1}{\partial x_1} + 2\frac{\partial \tilde{u}_2}{\partial x_2})\right) = 0. \tag{3.3}$$

However, this procedure is not quite justifiable since it has been implicit in our derivation that the curvature effects enter the model at lowest order. In order to model sheets which are planar or nearly planar, it is necessary to perform the asymptotic analysis of § 2.3 again in the crucial parameter regime when the curvature is of $O(\varepsilon)$. For pressure-driven flow of a sheet with $O(1)$ curvature, the tangential velocities are of $O(1)$ compared to the normal velocities. However, if a transverse pressure is applied to a nearly planar sheet, the enhanced normal velocities demand a rescaling that invalidates (3.1)–(3.3). Despite the fact that fixed Cartesian coordinates can be used for this analysis, the asymptotic reduction is complicated and the details

can be found in Howell (1995) where a system of equations is derived that generalizes the one-dimensional equations of Buckmaster *et al.* (1975). This system implies that nearly flat sheets are much more susceptible to tangential stretching than sheets with $O(1)$ curvature in the sense that a curved sheet will in general be able to respond to applied stress via a deformation of its centre-surface, while a nearly flat sheet is forced to stretch. Indeed, if the imposed tangential stretching is sufficient (the velocity gradients need to be at least of order $\Delta P/(\varepsilon^2 M)$) that the normal velocity is smaller than the tangential velocities by a factor of ε, then (3.1)–(3.3) can be rescued, albeit with scalings different from (2.12); this too is described in Howell (1995) where the complementary equation for the displacement of the centre-surface is also given.

3.2. *Axisymmetric sheets*

The viscous shell equations may be simplified considerably if the sheet under consideration is axisymmetric, so that the lines of curvature are the meridians and parallels. The velocity may, however, have both axial and azimuthal components. We parametrize the centre-surface by arclength $s(=x_1)$ and polar angle $\theta(=x_2/L)$:

$$\boldsymbol{r}_c = \begin{pmatrix} R(s,t)\cos\theta \\ R(s,t)\sin\theta \\ z(s,t) \end{pmatrix}, \text{ where } \mathrm{d}s^2 = \mathrm{d}R^2 + \mathrm{d}z^2. \tag{3.4}$$

The scaling factors and principal curvatures are then given by

$$a_s = 1, \quad a_\theta = R, \quad \kappa_s = -\left[1 - \left(\frac{\partial R}{\partial s}\right)^2\right]^{-1/2} \frac{\partial^2 R}{\partial s^2}, \quad \kappa_\theta = \frac{1}{R}\left[1 - \left(\frac{\partial R}{\partial s}\right)^2\right]^{1/2}. \tag{3.5}$$

We suppose all variables are independent of θ. Denoting by u_s and u_θ the fluid velocity components in the s– and θ–directions relative to the moving centre-sheet, the equations of motion may be written in the form

$$\frac{\partial}{\partial t}(Rh) + \frac{\partial}{\partial s}(u_s Rh) = 0, \tag{3.6}$$

$$\kappa_s \bar{\sigma}_{ss} + \kappa_\theta \bar{\sigma}_{\theta\theta} = \Delta P, \tag{3.7}$$

and

$$\frac{\partial}{\partial s}(R^2 \kappa_\theta \bar{\sigma}_{ss}) = \Delta P . R \frac{\partial R}{\partial s}, \tag{3.8}$$

where the extensional and hoop stresses are given by

$$\bar{\sigma}_{ss} = \frac{2\mu h}{R}\left[2R\frac{\partial u_s}{\partial s} + \left(\frac{\partial R}{\partial t} + u_s \frac{\partial R}{\partial s}\right)\right], \tag{3.9}$$

$$\bar{\sigma}_{\theta\theta} = \frac{2\mu h}{R}\left[R\frac{\partial u_s}{\partial s} + 2\left(\frac{\partial R}{\partial t} + u_s \frac{\partial R}{\partial s}\right)\right]. \tag{3.10}$$

The azimuthal velocity u_θ satisfies a decoupled equation

$$\frac{\partial}{\partial s}\left(\mu R^2 h \frac{\partial u_\theta}{\partial s}\right) = 0. \tag{3.11}$$

It is easily verified that (3.6)–(3.10) reduce to the steady-state model of Pearson & Petrie (1970*a*, equations 16 and 17) if the time-derivatives are neglected and the viscosity is assumed constant. They also reduce, when linearized for small R, to the

model of Yarin *et al.* (1994) for the drawing of a hollow slender axisymmetric fibre; (3.7) becomes $\bar{\sigma}_{\theta\theta} = R\Delta P$ approximately and hence (3.8) and (3.10) reduce to

$$\frac{\partial}{\partial s}\left(3\mu Rh\frac{\partial u_s}{\partial s}\right) = 0, \quad \Delta P.R = 2\mu h\left(\frac{\partial u_s}{\partial s} + \frac{2}{R}\left(\frac{\partial R}{\partial t} + u_s\frac{\partial R}{\partial s}\right)\right),$$

respectively, where we have a Trouton viscosity 3μ characteristic of axisymmetric fibre drawing. It is also interesting to consider the formal limit as $R \to \infty$ while the derivatives of R remain bounded, in which case (3.6)–(3.10) reduce to the model for a purely two-dimensional sheet (which we will describe further in § 3.3). In this case the Trouton viscosity is found to be 4μ, which is typical for the stretching of planar sheets. Hence (3.6)–(3.10) show how the Trouton viscosity for a hollow fibre changes from 3μ to 4μ depending on the geometry (see Howell 1994 for further details).

We shall not discuss the solution of (3.6)–(3.10) in general but concentrate on two simple examples which can be solved explicitly.

3.2.1. *Circular cylinders*

Neglecting s-variations leads to the following pair of ordinary differential equations for the radius and thickness of a two-dimensional, cylindrical sheet:

$$\frac{\mathrm{d}}{\mathrm{d}t}(Rh) = 0, \quad \frac{\mathrm{d}R}{\mathrm{d}t} = \frac{R^2\Delta P}{4\mu h}. \tag{3.12}$$

With initial conditions $R(0) = R_0$, $h(0) = h_0$ and for constant ΔP and μ, these are readily solved to give

$$R = R_0\left(1 - \frac{R_0 t}{2\mu h_0}\right)^{-1/2}, \quad h = h_0\left(1 - \frac{R_0 t}{2\mu h_0}\right)^{1/2}, \tag{3.13}$$

so that the radius becomes infinite and the thickness vanishes in a finite time $t^* = 2\mu h_0/(R_0\Delta P)$.

Note that this problem can be solved exactly, without using the slenderness of the sheet, by simply solving the Stokes equations in cylindrical polar coordinates. This results in the system

$$\frac{\mathrm{d}}{\mathrm{d}t}(Rh) = 0, \quad \frac{\mathrm{d}R}{\mathrm{d}t} = \frac{\Delta P}{4\mu h}\left(R^2 - \frac{h^2}{4}\right), \tag{3.14}$$

with solution

$$R^2 = \frac{R_0 h_0}{2}\coth\left(\frac{\Delta P}{4\mu}(t^* - t)\right), \quad h^2 = 2R_0 h_0 \tanh\left(\frac{\Delta P}{4\mu}(t^* - t)\right), \tag{3.15}$$

where the blow-up time is now given by

$$t^* = \frac{4\mu}{\Delta P}\tanh^{-1}\left(\frac{h_0}{2R_0}\right). \tag{3.16}$$

The simple solution found above is clearly the leading-order term of this exact solution as $h_0/R_0 \to 0$.

We have shown that the radius of a circular fluid sheet will become infinite in finite time under a constant pressure drop. Physically this happens because the applied pressure generates a force proportional to the radius which must be balanced by the normal stress which is proportional to the product of the thickness and the strain rate $\dot{R}/R$; meanwhile the radius has to be inversely proportional to the thickness in

order to conserve mass. However, maintaining a constant pressure drop as the volume inside the sheet becomes large may not be physically realizable and it is more realistic to prescribe the mass of gas inside the sheet as a function of time, and assume a gas law to give the pressure; it is easy to show that the radius will then remain finite.

3.2.2. *Spheres*

Another axisymmetric surface for which an explicit solution of the viscous shell equations can be found is a sphere. Assuming radial symmetry, the radius and thickness now satisfy

$$\frac{\mathrm{d}}{\mathrm{d}t}(R^2h) = 0, \quad \frac{\mathrm{d}R}{\mathrm{d}t} = \frac{R^2\Delta P}{12\mu h}, \tag{3.17}$$

and hence are given by

$$R = R_0\left(1 - \frac{R_0\Delta P t}{4\mu h_0}\right)^{-1/3}, \quad h = h_0\left(1 - \frac{R_0\Delta P t}{4\mu h_0}\right)^{2/3}. \tag{3.18}$$

The blow-up time is $4\mu h_0/(R_0\Delta P)$. In this case, the exact solution of the radially symmetric Stokes equations is given implicitly by

$$(R + \tfrac{1}{2}h)^3 - (R - \tfrac{1}{2}h)^3 = (R_0 + \tfrac{1}{2}h_0)^3 - (R_0 - \tfrac{1}{2}h_0)^3 = V \tag{3.19}$$

say, and

$$(R + \tfrac{1}{2}h)^3 = \frac{V}{\mathrm{e}^{3\Delta P(t^*-t)/4\mu} - 1}, \quad \text{with } t^* = \frac{4\mu}{\Delta P}\tanh^{-1}\left(\frac{h_0}{2R_0}\right). \tag{3.20}$$

3.3. *General cylindrical sheets*

Numerical calculations for a sheet without axial symmetry have been made by Burley & Graham (1991), Graham *et al.* (1992). If the sheet is flat in the x_2-direction we may simplify the viscous shell equations by setting

$$a_1 = a_2 = 1, \quad \kappa_2 = \tilde{u}_2 = v_2 = \frac{\partial}{\partial x_2} = 0.$$

The choice $a_1 = 1$ means that x_1 may be identified with arclength s, and the equations become

$$\frac{\partial h}{\partial t} + \frac{\partial}{\partial s}(\tilde{u}_1 h) = 0, \tag{3.21}$$

$$4\mu h\kappa_1\frac{\partial \tilde{u}_1}{\partial s} + \Delta P = 0, \tag{3.22}$$

$$\frac{\partial}{\partial s}\left(4\mu h\frac{\partial \tilde{u}_1}{\partial s}\right) = 0. \tag{3.23}$$

Without an applied pressure we find either $\kappa_1 = 0$ or $\tilde{u}_1 = 0$. In the first case where the sheet is straight, the equations are the same as for the drawing of a slender fibre, the time-dependent Trouton equations for viscous flow (Dewynne *et al.* 1989). In the second case, $h_t = 0$ and it is necessary to proceed further with the expansions to find an expression for κ_1. This latter case has been considered by Buckmaster *et al.* (1975) for a curved viscous fibre constrained to move in a plane and we will say more about this in the conclusion. However, when the pressure drop is included it is unnecessary to proceed any further with the expansions. Indeed, (3.22) and (3.23) imply

$$\frac{\partial \kappa_1}{\partial s} = 0, \tag{3.24}$$

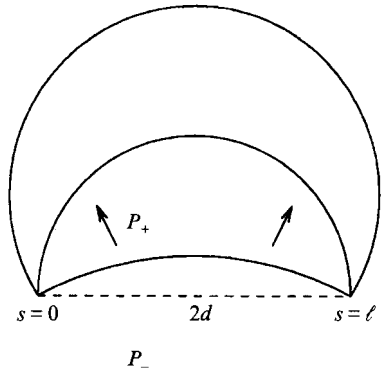

FIGURE 1. Extension of a two-dimensional thin sheet held at the ends.

so the curvature is uniform and hence the sheet must form a circular arc. Then h and $\tilde{u}_1$ satisfy the Trouton model:

$$\frac{\partial h}{\partial t} + \frac{\partial}{\partial s}(\tilde{u}_1 h) = 0, \quad h\frac{\partial \tilde{u}_1}{\partial s} = a(t), \tag{3.25}$$

where $a(t)$, the scaled tension in the sheet, is given in terms of the radius R of the arc formed by the sheet:

$$a(t) = R\Delta P/4\mu. \tag{3.26}$$

In the axisymmetric case these equations reduce to (3.12), which is easily retrieved when employing fixed (polar) coordinates.

Suppose the sheet is fixed at its two ends and blown out under an applied pressure drop; see figure 1. This configuration has been the subject of a numerical study (Graham *et al.* 1992) and is the prototype for more realistic models of industrial blowing processes (Pearson 1985, §20.1). The initial and boundary conditions to the equations (3.25) read

$$h(s,0) = h_0(s), \quad \tilde{u}_1(0,t) = 0, \quad \tilde{u}_1(\ell(t),t) = \dot{\ell}(t). \tag{3.27}$$

The governing equations (3.25) and boundary conditions (3.27) are identical to the fibre-drawing problem considered by Dewynne *et al.* (1989), in which the length ℓ is assumed to be a given function of t. However, for our pressure-driven extension the growth of ℓ is yet to be determined via the extra relation (3.26) which gives the tension a as a function of radius R, which is in turn a function of ℓ. Indeed, it is easily seen that R and ℓ are related by

$$\ell = \begin{cases} 2R\sin^{-1}(d/R) & \text{for } 2d \leqslant \ell \leqslant \pi d, \\ 2R\left[\pi - \sin^{-1}(d/R)\right] & \text{for } \pi d \leqslant \ell < \infty. \end{cases} \tag{3.28}$$

A plot of R against ℓ is shown in figure 2, with a minimum $R = d$ at $\ell = \pi d$ when the sheet is semicircular.

In Dewynne *et al.* (1989) it is shown that, with a partial hodograph transform (3.25) can be reduced to an ordinary differential equation for the thickness h:

$$h_s = hF(h + T) \tag{3.29}$$

where the function F is determined by the initial condition $h_0(s)$, from $h_{0s} = h_0F(h_0)$ and T is given by

$$T = -h(0,T) + h_0(0) = -h(\ell(T),T) + h_0(\ell_0). \tag{3.30}$$

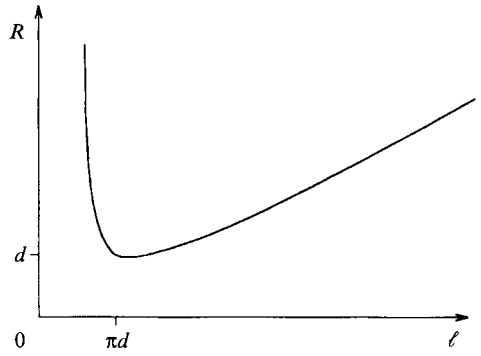

FIGURE 2. The sheet radius as a function of its length.

The ordinary differential equation (3.29) shows immediately that the layer of fluid cannot break if the function F is Lipschitz continuous, but the film can break if there is a cusp in $h_0(s)$ or if the film becomes infinitely long (which will happen in finite time). In the present problem the solution is complicated by the fact that ℓ is not known in advance. As in Pearson (1985, §20.2), this difficulty can be circumvented by transforming the problem into the Lagrangian variables ξ and τ satisfying $\chi(\xi,\tau) = s$, $\tau = t$, with

$$\chi_\tau(\xi,\tau) = \tilde{u}_1(s,t), \quad \chi(\xi,0) = \xi, \quad \chi(0,\tau) = 0, \quad \chi(1,\tau) = \ell(t). \tag{3.31}$$

We have scaled in such a way that the length of the sheet is initially 1. Then (3.25) gives

$$h_\tau + \frac{h}{\chi_\xi}\chi_{\tau\xi} = 0,$$

which may be integrated to give

$$\frac{\partial\chi}{\partial\xi} = \frac{h_0(\xi)}{h(\xi,\tau)}, \quad \text{or} \quad \chi(\xi,\tau) = \int_0^\xi \frac{h_0(\xi')\,\mathrm{d}\xi'}{h(\xi',\tau)}. \tag{3.32}$$

From (3.25) it follows that $h_\tau = a(\tau)$ and we may write

$$h(\xi,\tau) = h_0(\xi) - f(\tau), \tag{3.33}$$

where f satisfies

$$\dot{f}(\tau) = a(\tau) = \frac{R\Delta P}{4\mu}, \quad f(0) = 0. \tag{3.34}$$

Here R is related to ℓ by (3.28) and ℓ to f by

$$\ell(\tau) = \int_0^1 \frac{h_0(\xi)\,\mathrm{d}\xi}{h_0(\xi) - f(\tau)} = 1 + f(\tau)\int_0^1 \frac{\mathrm{d}\xi}{h_0(\xi) - f(\tau)}. \tag{3.35}$$

Once f is known, $h(s,t)$ is found from (3.33) and (3.32).

Now we have to solve the integrodifferential equation (3.34) for f which is complicated by the awkward implicit form (3.28). However, some interesting results about the asymptotic behaviour of f, and hence R, h and ℓ, may be obtained using approximations for $R(\ell)$. Of particular interest is the behaviour of the sheet when it is close to break-up, that is when f is close to the minimum value of h_0, say $h_0(b)$ and the length of the sheet is large. With d/ℓ small we can use $R \sim (\ell/2\pi)(1 + 2(d/\ell) + O(d/\ell)^3)$. Assume $h_0''(b)$ exists and is non-zero, then the asymptotic form of ℓ as a function of

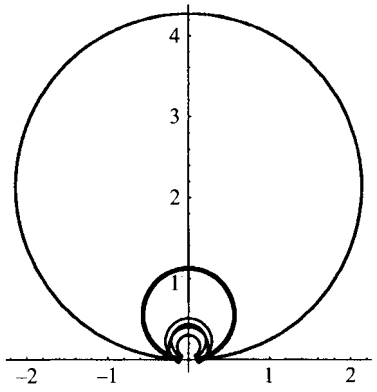

FIGURE 3. The blow-up behaviour of a cylindrical sheet with $\ell_0 = 1$, $d = 0.1$, $\mu = 1$ and applied pressure $\Delta P = 1$. Times shown: $t = 0.0, 0.5, 1.0, 1.1$.

the minimum thickness $h_m = h(b, \tau)$ is found to be

$$\ell \sim \pi h_0(b) \left(\frac{2}{h_0''(b) h_m} \right)^{1/2} \quad \text{as} \quad h_m \to 0, \tag{3.36}$$

and the leading-order solution of (3.34) reveals that the minimum thickness goes to zero like

$$h_m \sim \frac{1}{4} \left(\frac{9 \Delta P^2 h_0(b)^2}{2 \mu^2 h_0''(b)} \right)^{1/3} (\tau^* - \tau)^{2/3}, \tag{3.37}$$

while the radius goes to infinity like

$$R \sim \left(\frac{4 \mu h_0(b)^2}{3 \Delta P \, h_0''(b)} \right)^{1/3} (\tau^* - \tau)^{-1/3}. \tag{3.38}$$

We thus find that a smooth variation in the initial thickness changes the time-behaviour near blow-up from $R \sim (\tau^* - \tau)^{-1/2}$ for a uniform initial thickness (cf. (3.13)) to $R \sim (\tau^* - \tau)^{-1/3}$. If ΔP is constant the blow-up time is given by

$$\tau^* = \frac{4 \mu}{\Delta P} \int_0^{h_0(b)} \frac{\mathrm{d}f}{R(\ell(f))}, \tag{3.39}$$

which is finite since $R \geqslant \frac{1}{2}$. Figures 3 and 4 show examples of the blow-up of sheets with different initial thicknesses but with the same initial volumes.

4. Discussion and conclusions

A wide variety of industrially relevant pressure-driven liquid sheet flows are governed by a balance between the viscous stresses and the applied pressure. For such flows, we have derived the leading-order equations governing the dynamics of a sheet of arbitrary geometry. It is easy to see that our model (2.35)–(2.41) reduces to the equations (16)–(17) of the pioneering work of Pearson & Petrie (1970*a*) in the steady, axisymmetric case and to the evolution model of Yarin *et al.* (1994) in the axisymmetric case. The only discrepancy that we have found is that when the viscosity is non-constant, our procedure would give a model different from that in Pearson & Petrie (1970*a*) in that a term involving the derivative of the viscosity appears in our analogue of Pearson & Petrie's equation (17). All these models have

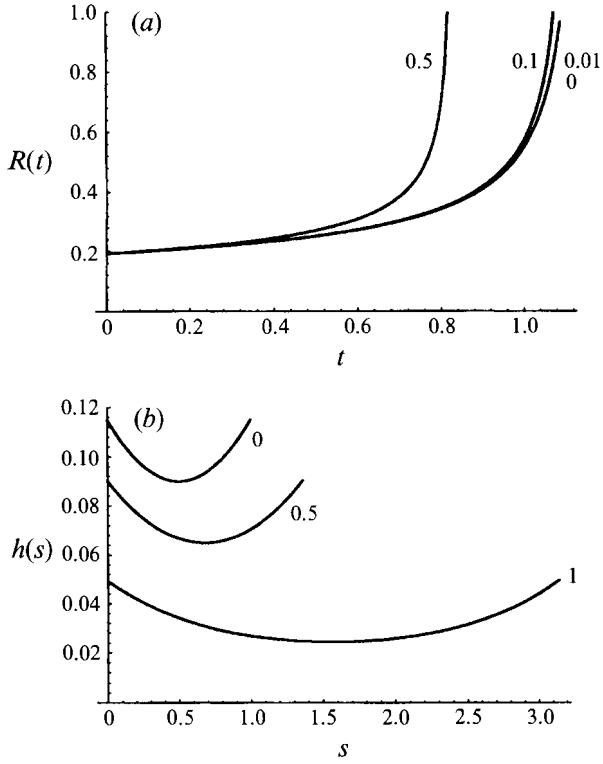

FIGURE 4. (*a*) The blow-up behaviour of the radius $R(t)$ is shown for initial thickness of the sheet given by $h_0(s) = 0.1 + \delta(s^2 - s + \frac{1}{6})$ and $\delta = 0.5, 0.1, 0.01, 0$. Again $\ell_0 = 1$, $d = 0.1$, $\mu = 1$ and $\Delta P = 1$. The change in thickness is shown in (*b*) for $\delta = 0.1$, $t = 0, 0.5, 1$.

a strong analogy with the shell equations of linear elasticity except that for viscous liquids the geometry can change substantially with time. In cases where the form of the geometry is preserved some analytical progress can be made, such as for a strictly two-dimensional sheet.

Of particular interest for the bottle-blowing problem is the evolution of a viscous sheet under an applied pressure drop. The simple analytical examples described suggest that such a sheet is likely to undergo finite-time blow-up if the pressure drop is held constant. The form taken by this blow-up is strongly dependent upon non-uniformities in the sheet thickness.

In many situations the effects of surface tension, gravity and inertia are small but we have indicated how they can be incorporated in the Appendix. In physical situations the viscosity μ will be a prescribed function of the temperature, which must be found from a coupled heat transfer equation. For simplicity we have only pursued the isothermal case. However, we note that the case in which μ is convected faithfully with the flow may be covered by our analysis by rescaling h with μ. Finally, another generalization of the model that has not been incorporated concerns the case when contact is made with a fixed surface, such that three phases – molten glass, air and a mould – meet at one particular line, and the model has to be extended to cover the different boundary conditions and the behaviour of the contact line; this configuration has been considered in Pearson (1985, §20.2).

Paradoxically, as mentioned in § 3.1 the most complicated parameter regimes that we have considered are those where the sheet is nearly flat. This situation can be clarified

by recalling the modelling of sheets which are not pressure-driven but only respond to prescribed boundary motion U, say. There, as shown for purely two-dimensional flow in Buckmaster *et al.* (1975), a sheet with $O(1)$ curvature undergoes negligible stretching and responds on a timescale L/U. Moreover, when the curvature is $O(\varepsilon)$ or less then, as shown in Wilmott (1989), a two-dimensional sheet stretches according to the extensional flow model (3.21)–(3.23) (with $\Delta P = 0$), also on a timescale L/U. In this latter case, an initially curved centre-line straightens on a shorter timescale $\varepsilon^2 L/U$; moreover, as shown in Buckmaster *et al.* (1975) and Wilmott (1989), the motion on the shorter timescale exhibits stability and reversibility properties quite different from those of (3.21)–(3.22), and much more like those of the inextensional model of Buckmaster *et al.* (1975).

Our assumption that the flow is entirely pressure-driven implies that even the $O(1)$ curvature motion is still described by an extensional flow model, albeit of a more general character than that for a two-dimensional sheet. An illustration of behaviour analogous to that found by Buckmaster *et al.* (1975) is the immediate adoption of a circular centre-line geometry in (3.23). However, from the preceding discussion, it is clear that short timescale motions even of $O(1)$ curvature configurations are possible, for which the model is quite different from that of § 2. An example would be the blow-out problem of figure 1 with a non–circular initial configuration. It seems likely (although unproven to our knowledge) that any curved surface will respond over a short timescale to an applied pressure drop via an isometric deformation – one in which no stresses are induced in the fluid sheet – followed on a longer timescale by an extensional flow. We conjecture that over the short timescale the sheet will assume the shape which maximizes the volume enclosed inside the sheet, over all surfaces which are isometric to the initial shape of the sheet. This conjecture is clearly a generalization of our result that over a short timescale, a two-dimensional sheet subjected to a pressure drop forms a circular arc – the configuration that maximizes the area which may be enclosed without altering the length of the sheet.

We would like to thank Mr D. Gelder of Pilkington Group Research and Dr D. M. Burley for many helpful discussions. We are grateful for the financial support of EPSRC (P.D.H.) and HCM (B.W.vdF.).

Appendix. Surface tension, gravity and inertia effects

If we are to include surface tension, gravity or inertia effects in the model, we need to make an assumption about the relative size of the coefficients. For instance, for an extremely slender film, such as a lamella in a foam, we may expect the geometry to be dominated by surface effects; such an application has been considered by Ida & Miksis (1995).

A.1. *Surface tension*

In order to model surface tension effects we will scale the dimensionless surface tension coefficient with ε and assume

$$\gamma^* = \frac{\gamma}{L\Delta P} = O(1).$$

After this scaling, the viscous shell equations (2.35)–(2.41) are unchanged except for the normal force balance (2.35) which becomes

$$\kappa_1(\bar{\sigma}_{11} + \gamma^*) + \kappa_2(\bar{\sigma}_{22} + \gamma^*) + \Delta P = 0. \tag{A 1}$$

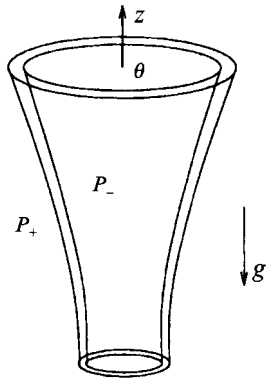

FIGURE 5. Extrusion of a cylindrical sheet under the influence of gravity.

As an example of the stabilizing effect of surface tension, we consider the evolution of a two-dimensional viscous sheet with surface tension.

It was found in § 3.3 that an inertia-free, slender two-dimensional viscous sheet will always form a circular arc under an applied pressure drop. This property is preserved when surface tension effects are included, and the only effect on the Trouton model of § 3.3 is to change the tension equation (3.34) to

$$\dot{f} = \frac{R\Delta P - \gamma^*}{4\mu}, \quad f(0) = 0. \tag{A 2}$$

As a result of this, if $\gamma^* > d\Delta P$ then there exists a stable steady state at which $\dot{f} = 0$ and surface tension balances the pressure drop.

A.2. *Gravity*

To model the extrusion of a sheet under the influence of gravity we impose a body force in the negative z-direction (figure 5), and, in order to balance gravity and viscous stresses, we scale the dimensionless parameter St with ε:

$$St = \frac{\rho g L}{\Delta P} = O(1).$$

For example, when studying a cylindrical sheet including gravity acting on it, the equations (3.7), (3.8) are changed to

$$\kappa_s \bar{\sigma}_{ss} + \kappa_\theta \bar{\sigma}_{\theta\theta} = \left(St\, h \frac{\partial R}{\partial s} + \Delta P \right), \tag{A 3}$$

and

$$\frac{\partial}{\partial s}(R^2 \kappa_\theta \bar{\sigma}_{ss}) = St\, Rh + \Delta P\, R \frac{\partial R}{\partial s}. \tag{A 4}$$

A.3. *Inertia effects*

In a typical glass-blowing process, inertia effects are only likely to be important if the process is very fast or if the glass is very hot. In order to include inertia effects in the viscous shell equations, it is necessary to calculate the acceleration vector of the fluid. This may be done using the convective derivative (2.26) and noting that, for a vector field $\boldsymbol{V}$,

$$\frac{\mathrm{D}\boldsymbol{V}}{\mathrm{D}t} = \frac{\partial \boldsymbol{V}}{\partial t} + \frac{\partial \boldsymbol{V}}{\partial x_i} \frac{\mathrm{D}x_i}{\mathrm{D}t},$$

where the sum is from $i = 1$ to 3. Employing the leading-order equations of § 2.3, the leading-order components of the acceleration vector are given by (dropping superscripts)

$$\boldsymbol{n}\cdot\frac{\mathrm{D}\boldsymbol{u}}{\mathrm{D}t}\sim\frac{\partial v_3}{\partial t}+\frac{\tilde{u}_1}{a_1}\frac{\partial v_3}{\partial x_1}+\frac{\tilde{u}_2}{a_2}\frac{\partial v_3}{\partial x_2}+\kappa_1 u_1^2+\kappa_2 u_2^2+\frac{u_1}{a_1}\frac{\partial v_3}{\partial x_1}+\frac{u_2}{a_2}\frac{\partial v_3}{\partial x_2}+O(\varepsilon), \tag{A 5}$$

$$\boldsymbol{e}_1\cdot\frac{\mathrm{D}\boldsymbol{u}}{\mathrm{D}t}\sim\frac{\partial u_1}{\partial t}+\frac{\tilde{u}_1}{a_1}\frac{\partial u_1}{\partial x_1}+\frac{\tilde{u}_2}{a_2}\frac{\partial u_1}{\partial x_2}-v_3\left(\kappa_1 u_1+\frac{1}{a_1}\frac{\partial v_3}{\partial x_1}\right)+\frac{u_2}{a_2}\left(\frac{\partial v_1}{\partial x_2}+\frac{\tilde{u}_1}{a_1}\frac{\partial a_1}{\partial x_2}-\frac{u_2}{a_1}\frac{\partial a_2}{\partial x_1}\right)+O(\varepsilon), \tag{A 6}$$

$$\boldsymbol{e}_2\cdot\frac{\mathrm{D}\boldsymbol{u}}{\mathrm{D}t}\sim\frac{\partial u_2}{\partial t}+\frac{\tilde{u}_1}{a_1}\frac{\partial u_2}{\partial x_1}+\frac{\tilde{u}_2}{a_2}\frac{\partial u_2}{\partial x_2}-v_3\left(\kappa_2 u_2+\frac{1}{a_2}\frac{\partial v_3}{\partial x_2}\right)+\frac{u_1}{a_1}\left(\frac{\partial v_2}{\partial x_1}+\frac{\tilde{u}_2}{a_2}\frac{\partial a_2}{\partial x_1}-\frac{u_1}{a_2}\frac{\partial a_1}{\partial x_2}\right)+O(\varepsilon). \tag{A 7}$$

The viscous shell equations are modified to take account of inertia by replacing ΔP in (2.35) by $\Delta P - Re\, h\boldsymbol{n}\cdot\mathrm{D}\boldsymbol{u}/\mathrm{D}t$ and by adding $-Re\, a_1 a_2 h\boldsymbol{e}_i\cdot\mathrm{D}\boldsymbol{u}/\mathrm{D}t$ for $i = 1, 2$ in the left-hand sides of (2.40) and (2.41).

For example, the equations for a two-dimensional sheet used in § 3.3 become

$$\frac{\partial h}{\partial t}+\frac{\partial}{\partial s}(\tilde{u}_1 h)=0, \tag{A 8}$$

$$4\mu\kappa_1 h\frac{\partial\tilde{u}_1}{\partial s}=\Delta P+Re\, h\left(\frac{\partial v_3}{\partial t}+(2u_1-v_1)\frac{\partial v_3}{\partial s}+\kappa_1 u_1^2\right), \tag{A 9}$$

$$\frac{\partial}{\partial s}\left(4\mu h\frac{\partial\tilde{u}_1}{\partial s}\right)=Re\, h\left(\frac{\partial u_1}{\partial t}+\tilde{u}_1\frac{\partial u_1}{\partial s}-\kappa_1 u_1 v_3-v_3\frac{\partial v_3}{\partial s}\right), \tag{A 10}$$

where

$$\frac{\partial v_1}{\partial s}=\kappa_1 v_3\quad\text{and}\quad\frac{\partial\kappa_1}{\partial t}=\frac{\partial}{\partial s}\left(\frac{\partial v_3}{\partial s}+\kappa_1 v_1\right). \tag{A 11}$$

The inclusion of inertia makes the equations much harder to solve. In particular, the property found in § 3.3 that the sheet will always form a circular arc is lost here, and in general we must solve a coupled problem for the curvature.

REFERENCES

Aris, R. 1962 *Vectors, Tensors, and the Basic Equations of Fluid Mechanics.* Prentice–Hall (reprinted 1989 Dover).

Buckmaster, J. D. & Nachman, A. 1978 The buckling and stretching of a viscida II. Effects of surface tension. *Q. J. Mech. Appl. Maths* **31**, 157–168.

Buckmaster, J. D., Nachman, A. & Ting, L. 1975 The buckling and stretching of a viscida. *J. Fluid Mech.* **69**, 1–20.

Burley, D. M. & Graham, S. J. 1991 The blowing of thin films into moulds with applications in the glass container industry. *Math. Fin. Elem. Appl.* **7**, 279–286.

Cao, B. S. & Campbell, G. A. 1990 Viscoplastic–elastic modeling of tubular blown film processing. *AICHE J.* **36**, 420–430.

Dewynne, J. N., Howell, P. D. & Wilmott, P. 1994 Slender viscous fibres with inertia and gravity. *Q. J. Mech. Appl. Maths* **47**, 541–555.

DEWYNNE, J. N., OCKENDON, J. R. & WILMOTT, P. 1989 On a mathematical model for fibre tapering. *SIAM J. Appl. Maths* **49**, 983–990.

DEWYNNE, J. N., OCKENDON, J. R. & WILMOTT, P. 1992 Systematic derivation of the leading-order equations for extensional flows in slender geometries. *J. Fluid Mech.* **244**, 323–338.

GEYLING, F. T. 1976 Basic fluid dynamic considerations in the drawing of optical fibres. *Bell. Sys. Tech. J.* **55**, 1011–1056.

GEYLING, F. T. & HOMSY, G. M. 1980 Extensional instabilities of the glass fibre process. *Glass Tech.* **21**, 95–102.

GRAHAM, S. J. 1987 Mathematical modelling of glass flow in container manufacture. PhD thesis, University of Sheffield.

GRAHAM, S. J., BURLEY, D. M. & CARLING, J. C. 1992 Fluid flow in thin films using finite elements. *Math. Engng Ind.* **3**, 229–246.

GUPTA, R. K., METZNER, A. B. & WISSBRUN, K. F. 1982 Modeling of polymeric film-blowing processes. *Polymer Engng Sci.* **22**, 172–181.

HOWELL, P. D. 1994 Extensional thin layer flows. DPhil thesis, Oxford University.

HOWELL, P. D. 1995 Models for slender viscous sheets. *E. J. Appl. Maths* (submitted).

IDA, M. P. & MIKSIS, M. J. 1995 Dynamics of a lamella in a capillary tube. *SIAM J. Appl. Maths* **55**, 23–57.

KREYSZIG, E. 1959 *Differential Geometry*. University of Toronto Press (reprinted 1991 Dover).

LANDAU, L. D. & LIFSCHITZ, E. M. 1959 *Theory of Elasticity*. Pergamon.

LOVE, A. E. H. 1927 *A Treatise on the Mathematical Theory of Elasticity*. Cambridge University Press.

MATOVICH, M. A. & PEARSON, J. R. A. 1969 Spinning a molten thread line. *Indust. Engng Chem. Fundam.* **8**, 512–519.

PEARSON, J. R. A. 1985 *Mechanics of Polymer Processing*. Elsevier Applied Science.

PEARSON, J. R. A. & MATOVICH, M. A. 1969 Spinning a molten thread line. *Indust. Engng Chem. Fundam.* **8**, 605–609.

PEARSON, J. R. A. & PETRIE, C. J. S. 1970*a* The flow of a tubular film. Part 1. Formal mathematical representation. *J. Fluid Mech.* **40**, 1–19.

PEARSON, J. R. A. & PETRIE, C. J. S. 1970*b* The flow of a tubular film. Part 2. Interpretation of the model and discussion of solutions. *J. Fluid Mech.* **42**, 609–625.

ROSENHEAD, L. 1963 *Laminar Boundary Layers*. Clarendon.

SAXELBY, C. & AITCHISON, J. M. 1986 A numerical model of the glass sheet and fibre updraw process. In *Industrial Numerical Analysis* (ed. S. McKee & C. M. Elliot). Oxford University Press.

SCHULTZ, W. W. & DAVIS, S. H. 1982 One-dimensional liquid fibers. *J. Rheol.* **26**, 331–345.

SHAH, F. T. & PEARSON, J. R. A. 1972 On the stability of non-isothermal fibre spinning. *Indust. Engng Chem. Fundam.* **11**, 145–149.

TIMOSHENKO, S. P. & WOINOWSKY-KRIEGER, S. 1959 *Theory of Shells and Plates*. McGraw Hill.

WILMOTT, P. 1989 The stretching of a thin viscous inclusion and the drawing of glass sheets. *Phys. Fluids* A **7**, 1098–1103.

YARIN, A. L., GOSPODINOV, P. & ROUSSINOV, V. I. 1994 Stability loss and sensitivity in hollow-fiber drawing. *Phys. Fluids* **6**, 1454–1463.

YEOW, Y. L. 1976 Stability of tubular film flow: a model of the film-blowing process. *J. Fluid Mech.* **75**, 577–591.